X-ray-emission studies of chemical bonding in transition-metal silicides

P. J. W. Weijs,* H. van Leuken,† R. A. de Groot, and J. C. Fuggle
Research Institute for Materials, Faculty of Science, University of Nijmegen, Toernooiveld, NL-6525 ED Nijmegen, The Netherlands

S. Reiter and G. Wiech
Sektion Physik, Ludwig-Maximilians-Universität München, D-8000 München 22, Federal Republic of Germany

K. H. J. Buschow
Philips Research Laboratories, P.O. Box 80.000, NL-5600 JA Eindhoven, The Netherlands
(Received 9 April 1991)

We present Si $L_{2,3}$ emission-band spectra of a series of 3*d* and 4*d* transition-metal (TM) silicides, together wtih Si *K* emission-band spectra of four 3*d* TM disilicides. The data are compared with augmented-spherical-wave density-of-states (DOS) calculations, and good agreement is found. The trends we find are explained with a general scheme for chemical bonding in TM silicides. The differences between the experimental data and the calculated DOS curves are tentatively attributed to self-energy effects.

I. INTRODUCTION

The purpose of this paper is to present data on the soft-x-ray emission-band spectra of the silicon atoms in transition-metal (TM) silicides and to relate these data to density-of-states (DOS) calculations and to chemical bonding. The work is part of a more extensive project on the electronic structure of silicides,[1–8] and is to be seen in the context of the problem of the interactions at metal-silicon interfaces. It is our hope that study of the metal-silicon interactions in periodic lattices and chemical compounds will give more insight into the problematics of these technologically important interfaces. Our previous work related primarily to the photoemission and inverse photoemission which gave a picture of the total DOS above and below the Fermi level (E_F) and led to some quite detailed insight into bonding mechanisms, quasigaps, and hybridization between metal and silicon levels. The present work involving x-ray-emission spectroscopy (XES) gives more detailed information because of its site and symmetry selectivity; it relates directly to the partial DOS on the silicon atoms. This more detailed information on the partial DOS yielded by XES reinforces and also enhances the picture of the chemical interaction between the various atoms which has been built up by previous work.[1–13] We will show by comparison of the Si $L_{2,3}$ emission-band spectra with calculated DOS that states with both Si *s* and *d* character give a contribution to the spectrum and that in the case of $NiSi_2$ there is a significant Si *s* contribution right at E_F. By comparing the Si $L_{2,3}$ and Si *K* emission-band spectra, we will show the strong separation of Si *s* and *p* character in the total DOS. Finally, we will note significant differences between partial DOS, in particular Si *s* DOS, and the emission spectra. These differences, which have not been detected before, will be tentatively related to self-energy effects and we will discuss the point that similar effects must be taken into account in any computation of electronic structure of metal-silicon interfaces.

II. EXPERIMENT

The polycrystalline samples were prepared by indirect rf heating or by arc melting of transition metal and Si, in the correct stoichiometric proportion, in an atmosphere of purified argon. The structures were checked by x-ray diffraction to ensure that no samples were used with more than 3% of spurious phases. The samples were cut by spark erosion, scrubbed with silicon-free abrasive, and finally pulverized. The powdered silicides were pressed into a scratched copper plate which then was attached to the water-cooled sample holder, thus ensuring good thermal and electrical contact. In this way we prepared two samples of each silicide.

The Si $L_{2,3}$ emission bands were measured in first spectral order with a 2-m concave grating grazing incidence spectrometer, resulting in an energy resolution of ~0.2 eV at a photon energy of 90 eV. The spectra were excited by low-load electron bombardment (3 kV, 1 mA; area of focal spot about 15 mm^2) and recorded with a parallel-plate photoelectron multiplier.

During the course of the measurements no changes of the samples and the spectra due to electron bombardment were observed. The spectra of both samples of each silicide proved to be identical. After adding them, a linear background was subtracted.

The Si *K* emission bands were measured with a Johann-type spectrometer. The dispersing element was a quartz crystal, cut parallel to the $10\bar{1}0$ plane, and bent to a radius of about 110 cm. Fluorescence excitation was used, the x-ray tube being operated at 2 kW (10 kV, 200 mA; tungsten anode). The spectra were recorded with a position sensitive detector with a backgammon cathode.[14]

Where possible, the Fermi levels were determined by x-ray photoelectron spectroscopy (XPS) core-level peak positions from our own measurements ($TiSi_2$ and $CoSi_2$) or from literature (Ref. 13 for $CrSi_2$). The Si K end Si L emission bands were aligned to a common energy scale by the Si $K\alpha_1$ line:

$$E(\text{Si } K)-E(\text{Si } L_{2,3})=E(\text{Si } 1s)-E(\text{Si } 2p_{3/2})$$
$$=E(\text{Si } K\alpha_1)\ .$$

Since the energy of the Si $K\alpha$ lines of the silicides studied in this paper were not available we used the results given by Zöpf.[15] He studied a number of TM silicides and found that the energy of the Si $K\alpha_1$ lines of all these silicides is 1740.15±0.10 eV. This value was assumed to be valid also for other silicides. Using this procedure, good agreement with the calculated DOS was found in all cases.

III. COMPUTATION

The computational method used was an *ab initio*, self-consistent, scalar-relativistic, augmented-spherical-wave (ASW) method of Williams, Kübler, and Gelatt,[16] and was carried out for these silicides in their actual crystal structures. As basis functions for the 3*d*-metal silicide we used Si 3*s* and 3*p* ASW's on the Si site and 3*d*, 4*s*, and 4*p* ASW's on the metal site. The internal l summation was extended to $l=2$ for the Si and to $l=3$ for the metals. For the specific case of the 4*d* silicides we also included the Si 3*d* ASW's directly. Further details about the band-structure calculations are given elsewhere.[4] For Cr_5Si_3 and Cr_3Si, no calculated DOS were available.

In order to compare the theoretical data with our measurements, the local partial DOS were convoluted with Lorentzian and Gaussian distributions in order to account for the core and final-state lifetimes and for instrumental effects, respectively. The broadening parameters used were $0.5+0.12(E-E_F)$ eV full width at half maximum (FWHM) Lorentzian for Si K emission and $0.1+0.12(E-E_F)$ eV FWHM Lorentzian for Si $L_{2,3}$ emission.[17–20] In addition, in all cases a 0.3-eV FWHM Gaussian was used.

IV. RESULTS AND INTERPRETATION

Because of the dipole selection rule and the local nature of the x-ray-emission matrix element the Si $L_{2,3}$ band spectra are related primarily to the local density of $(s+d)$ states at the silicon site, and the Si K spectra are related primarily to the partial density of Si p states. Wherever possible in this paper we will present experimental data together with calculated partial DOS. However, one should note that there is not a one-to-one equivalence between partial DOS and spectra: first we name the single-particle transition matrix element which varies significantly, even within any one band.[21,22] Second, for the $L_{2,3}$ spectra there is the unknown factor weighting Si s with respect to Si d states (in absence of any information we will always present s and d states in a one-to-one ratio). Finally, we note the energy dependence of the self-energy effects or exchange-correlation terms. Briefly, this has a real part, producing shifts, and an imaginary part corresponding to damping and broadening features in the spectra. We will return to the discussion of self-energy effects in Sec. V H.

Our experimental spectra are presented in Figs. 1–4. In general, these results are in reasonable agreement with previously published spectra. (For Si spectra, see Refs. 23–26; $CoSi_2$, Refs. 26 and 27; $NiSi_2$, Refs. 26 and 28; $NbSi_2$, Refs. 15 and 29; $MoSi_2$, Ref. 30; Cr_3Si, Ref. 15; and Refs. 15, 25, 28, and 30–33 for various other silicides.) The $L_{2,3}$ emission bands (Figs. 1–3) are characterized by strong peaks centered between 7 and 10 eV below E_F, which are related to the peaks which have been observed in Si (Refs. 23–26) and other silicides[15,26,29,30] and have traditionally been assigned to a peak in the local density of Si s states. This assignment is confirmed by our calculated partial DOS, although we note that there are some differences between experiment and theory which are discussed in Sec. V H. The Si s peak shows subtle but definite changes in shape and position as a function of composition and d-band filling of the TM element. In addition the spectra show long plateaus or multiple peaks extending in many cases all the way up to the Fermi level. We will show that these plateaus have

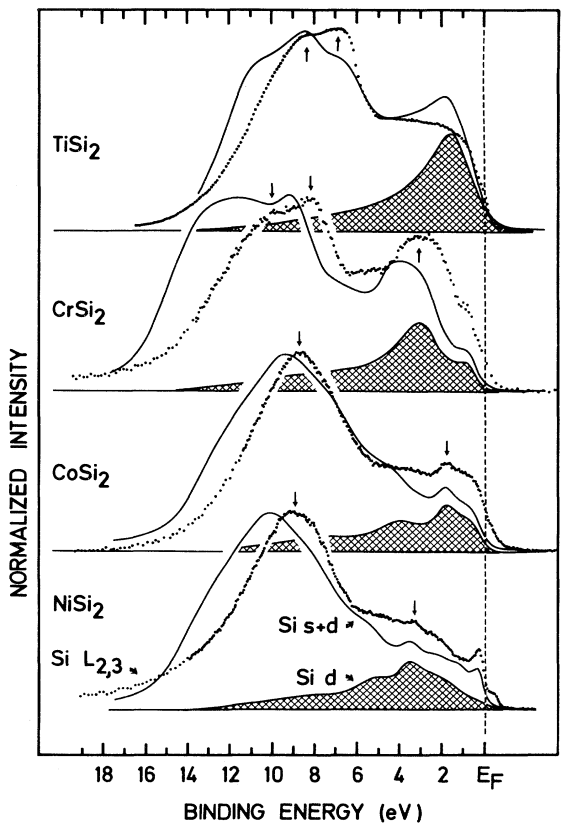

FIG. 1. Si $L_{2,3}$ emission-band spectra (dots) and calculated DOS of 3*d* TM disilicides. The Si $(s+d)$ DOS is given as a solid line, the Si d contribution to this curve is shaded. The arrows indicate the experimental peak position tabulated in Table I.

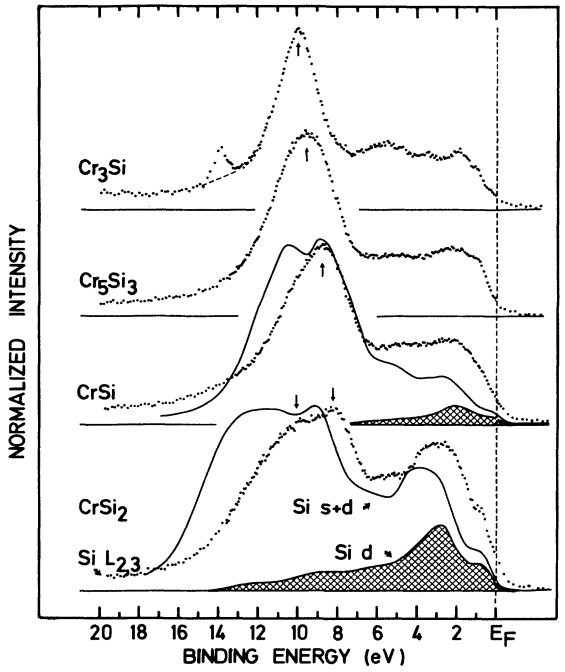

FIG. 2. Si $L_{2,3}$ emission-band spectra (dots) of four chromium silicides. For $CrSi_2$ and CrSi the Si $(s+d)$ DOS is given as a solid line, the Si d contribution to this curve is shaded. The arrows indicate the experimental peak positions tabulated in Table I.

contributions from Si s as well from Si d character. The spectral intensity is low in all cases. Exact peak positions for both calculated DOS and experimental data are given in Table I. The latter are indicated with arrows in Figs. 1–3.

Both the Si K emission bands and the partial DOS calculations indicate that the major weight of occupied Si p states is in a peak centered between 5 and 2 eV below E_F, again in agreement with other published data.[23,25,27–29] As indicated in Fig. 4, there is relatively little overlap between the Si p state density and the major Si s peak. Our Si K spectra also show significant structure in the peaks and small differences with respect to partial density of Si p state curves. Both items are discussed in Secs. V E and V H, respectively. For the exact peak positions we refer to Table II.

V. DISCUSSION

We have shown that the combination of XES and calculated DOS allows us to give a detailed picture of the distribution of the density Si s, p, and d states in the valence bands of various $3d$ and $4d$ TM silicides. We start our discussion with a detailed analysis of the Si $L_{2,3}$ emission band spectra (Secs. V A–V C) and the role of Si s states in chemical bonding (Sec. V D). This is followed by a similar discussion concerning the Si K emission-band spectra in Sec. V E. After this analysis of the spectra the influence of the TM d band on the Si sp state density is reviewed in Sec. V F, followed by the effect of different stoichiometries on the Si $L_{2,3}$ spectra (Sec. V G). Finally, Sec. V will be closed by a discussion about the differences we observe between the calculated DOS and the experimental spectra and these differences will be related to self-energy effects.

A. Contributions of Si s and Si d character to the $L_{2,3}$ emission-band spectra

As shown in Fig. 1 for the four $3d$ disilicides, the region between E_F and ~6-eV binding energy (BE) contains states with both Si s and Si d character so that both may contribute to the long plateau region of the $L_{2,3}$ spectra, in principle at least. We do not know the ratio of s to d matrix elements, but there are indications from the comparison of the DOS with the spectra that both Si s and Si d contribute with a weight quite similar to the partial state densities. These indications include the increase of weight W of the calculated Si d DOS in the series $W_{NiSi_2} \lesssim W_{CoSi_2} < W_{CrSi_2} < W_{TiSi_2}$. The shapes of the experimental curves do not agree with the shapes of the Si s DOS but look far more similar to the total Si $(s+d)$

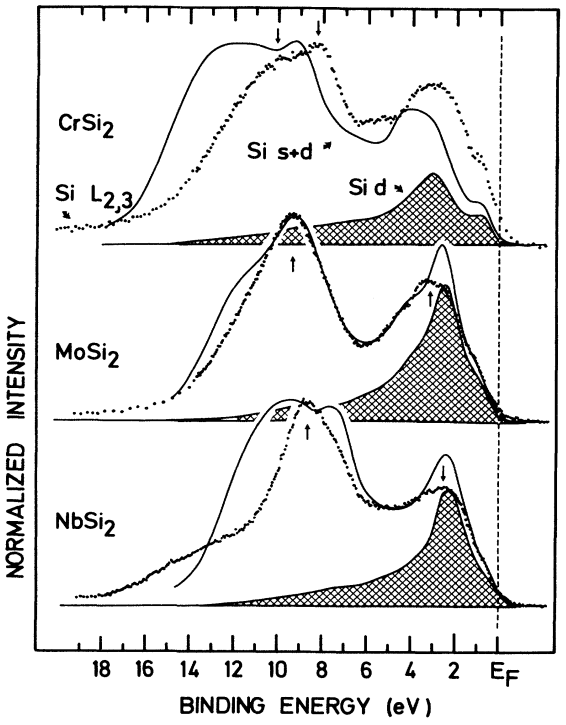

FIG. 3. Si $L_{2,3}$ emission band spectra (dots) and calculated DOS of $CrSi_2$, $MoSi_2$, and $NbSi_2$. The Si $(s+d)$ DOS is given as a solid line, the Si d contribution to this curve is shaded. The arrows indicate the experimental peak positions tabulated in Table I. (In the binding energy region 11–17 eV the strong Nb M_ζ line in second order is superimposed on the Si L spectrum of $NbSi_2$. The linear tail in that Si L band originates from the fact that the intensity of the Nb M_ζ line, which was subtracted from the measured spectrum, was chosen a bit too low.)

DOS. Also, it would require a very unusual variation with energy of the Si *s* matrix element for the contribution of the *s* states in this region to be totally suppressed. We thus proceed in the assumption that both the Si *s* and *d* states contribute to this region of the spectrum with a weight proportional to the partial DOS. Nevertheless, our knowledge of these relative matrix elements is imprecise and as peak positions predicted from the calculated DOS depend very strongly on the relative matrix elements, one should not use the difference between predicted and experimental peak positions in the low BE region to support conclusions about, e.g., self-energy contributions. Similar conclusions would be reached for similar reasons for CrSi, $MoSi_2$, and $NbSi_2$.

B. Links between Si *d* and TM *d* states

The observation of a contribution from Si *d* states to the occupied DOS of TM silicides and to the Si $L_{2,3}$ spectra leads us to ask what is the origin of this Si *d* state character. One could well understand that tails of the TM *d* wave functions might extend into the Si spheres and their symmetry might lead to *d* character at the Si sites. The discussion whether Si *d* character is intrinsic to the Si site or comes from the tails of wave functions centered at the neighboring site is partially academic because the wave function of the *d* state on the Si site will in both cases be determined by the potentials within the Si sphere. However, there are several indications in our data that the Si *d* is in some way linked to the TM *d* character. Two of these indications are contained in Figs. 1 and 3. In Fig. 1 we see that the relative weight of Si *d* increases from $NiSi_2$ to $TiSi_2$ and this could be linked to the more diffuse nature of the Ti *d* states which could lead to enhanced tailing on to the Si site.[34] Second, a similar trend is seen in Fig. 3, where the Si *d* contribution is much greater for the 4*d* silicides and the 4*d* orbitals are known to be more diffuse and even in the pure elements their bandwidths are much larger.[5]

To check this we have compared the Si *d* and TM *d* partial DOS for the four 3*d* disilicides in Fig. 5. We observe that the number of peaks and the overall shapes of the partial DOS curves for the metal *d* and the Si *d* are very similar in all four cases. This is a strong indication that the Si *d* is in some way linked to the tails of the TM *d* wave functions. It is also in accord with the decrease of the ratio of Si *d* to metal *d* in the sequence $TiSi_2 > CrSi_2 > CoSi_2 \gtrsim NiSi_2$, which would be expected from the decrease in the radii of the TM wave functions.[34]

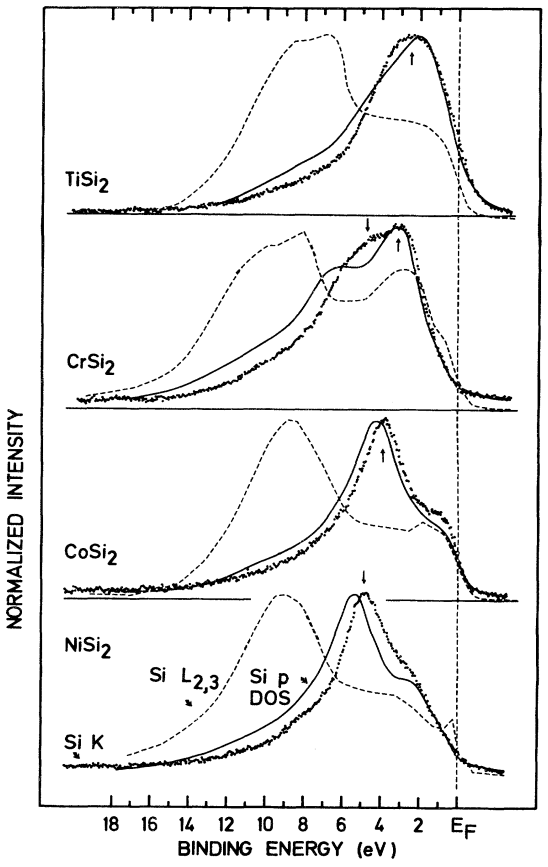

FIG. 4. Si *K* emission-band spectra (dots) and calculated Si *p* DOS (solid curve) of 3*d* TM silicides. Also shown are the Si $L_{2,3}$ emission spectra (dashed curves) from Fig. 1. The arrows indicate the experimental peak positions tabulated in Table II.

TABLE I. Binding energies (in eV) of valence-band features in the Si $L_{2,3}$ emission-band spectra and in the calculated DOS. In Figs. 1–3 the tabulated experimental peak positions are indicated with arrows.

Material	Expt.	DOS	Expt.	DOS	Expt.	DOS
$TiSi_2$		1.8	6.9	6.8	8.4	8.5
$CrSi_2$	3.1	4.0	8.2	9.3	10.1	12.0
$CoSi_2$	1.8	1.9	8.8	9.4		
$NiSi_2$	3.4	3.6	9.0	10.2		
Cr_3Si			9.9			
Cr_5Si_3			9.6			
CrSi			8.8	8.9		10.5
$MoSi_2$	3.1	2.6	9.4	9.3		
$NbSi_2$	2.5	2.4		7.6	8.6	9.5

TABLE II. Binding energies (in eV) of valence-band features in the Si *K* emission-band spectra and in the calculated DOS. In Fig. 4 the tabulated experimental peak positions are indicated with arrows.

Material	Expt.	DOS	Expt.	DOS
$TiSi_2$	2.5	2.1		
$CrSi_2$	3.1	3.1	4.7	6.0
$CoSi_2$	3.9	4.2		
$NiSi_2$	4.9	5.4		

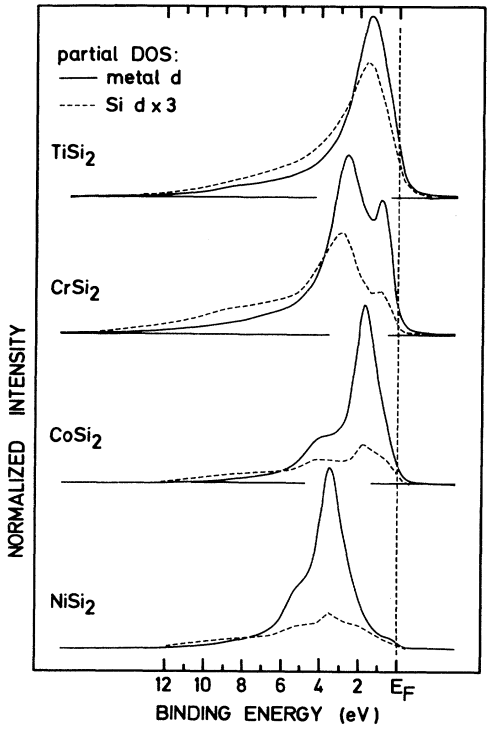

FIG. 5. Calculated TM *d* and Si *d* density of states. The Si *d* DOS is multiplied by 3.

C. The shape of Si *s* state peaks

All the Si $L_{2,3}$ emission-band spectra of silicides in Figs. 1–3 (and those of Si and silicides in the literature) show their major peak at ~10 eV below E_F. However, there are considerable differences between the shapes of these peaks in different silicides and also the calculated partial Si *s* DOS cures for different silicides show important differences. In addition, in many cases there are strong differences between the partial Si *s* DOS and Si $L_{2,3}$ band spectrum in the region of these peaks. For instance, the Si *s* DOS in $CrSi_2$ is shifted to higher BE with respect to the spectra in this region and there is a very strong broad peak at ~13 eV BE, which is very difficult to associate with any feature in the spectrum (see Fig. 1). Also CrSi (Fig. 2) and $NbSi_2$ (Fig. 3) show clear double-peak structures which have no analog in the observed spectra.

We certainly see changes in the partial DOS curves from one sample to another which may be associated with changes in crystal structures, which are tabulated in Table III. For instance, $CrSi_2$ and $NbSi_2$ have the same crystal structure and the calculations give similar double-peak structures. Also $CoSi_2$ and $NiSi_2$, which have the CaF_2 structure, show single broad peaks in both partial DOS and Si $L_{2,3}$ emission-band spectra. However, the present state of disagreement between experiment and theory is such that no other generalizations are justified. The differences between experiment and theory, for many silicides in this region, may be due to self-energy effects, but even this explanation is not totally satisfactory, as discussed in Sec. V H.

D. The role of Si *s* states in bonding

We have summarized elsewhere the long history of the discussion of the role of the Si *s* states.[4] Briefly, there are two extreme models, one involving sp^3 hybrids, so that there is a whole Si *s* electron contribution to the bond order, and a second extreme model in which the Si configuration is s^2p^2 and Si *s* electrons do not contribute to the bond order at all. Elsewhere[4] we argued mainly on the basis of DOS calculations that there were ~1.6 Si *s* electrons per Si atom and hence the Si *s* states contribute ~0.4 electrons to the bond order. We will show that the data we have now accumulated are an experimental confirmation of this conclusion.

On the one hand, we always see a strong Si *s* peak (or a double-peak structure) at the bottom of the band, in both DOS and the $L_{2,3}$spectra, where there is virtually no Si *p* state density. This argues strongly against the Si sp^3 hybrid model. On the other hand, however, we also found Si *s* state density extending right up to the Fermi level, and even beyond, in all the calculations. Furthermore, the spectra could only be satisfactorily interpreted if we assume a Si *s* contribution to the spectra extending all the way to up E_F. This supports the argument that there is at least some Si *s* character to the bond order and cohesive energy. In addition, there is a very interesting little peak at E_F in $NiSi_2$ (Fig. 1) which, according to the calculations, should be attributed to Si *s* state density. This little peak was also found by Nakamura *et al.*[26]

TABLE III. Crystal structures and nearest-neighbor distances in the TM disilicides, given in angstroms. The number of nearest neighbors are given in parentheses.

Material	Crystal structure	TM-Si	TM-TM	Si-Si	Ref.
$TiSi_2$	*C*54 ($TiSi_2$)	2.54(4)	3.2(4)	2.54(2)	44
$CrSi_2$	*C*40 ($CrSi_2$)	2.47(4)	3.06(4)	2.47(2)	45
$CoSi_2$	*C*1 (CaF_2)	2.32(8)		2.68(6)	46
$NiSi_2$	*C*1 (CaF_2)	2.34(8)		2.7(6)	46
CrSi	*B*20 (FeSi)	2.31(1)	2.83(6)	2.85(6)	47
Cr_5Si_3	*T*1 (W_5Si_3)	2.43(6)	2.32(2)	2.32(2)	48
Cr_3Si	*A*15 (βW)	2.55(4)	2.28(2)		48
$NbSi_2$	*C*40 ($CrSi_2$)	2.60(4)	3.25(4)	2.60(2)	49
$MoSi_2$	CaC_2 ($MoSi_2$)	2.615(8)	3.2(4)	2.615(4)	50

The fact that Si s DOS has significant weight at E_F was first claimed by a nuclear-magnetic-resonance study.[35] Even without an analysis of the phases of the wave functions, we may attribute this peak to the beginning of bands in which the Si s contribution is antibonding. It is not seen in the other silicides we have investigated because it occurs above the TM d band and the TM d bands of the other silicides are not completely filled.

The above arguments lead us to conclude that the true situation in the silicides we have studied is intermediate between the sp^3 configuration of pure silicon, and the s^2p^2 ground state of the free atom. However, it is closer to the s^2p^2 limit and we estimate it on the basis of DOS calculations to be $s^{1.6}p^{2.4}$.

E. The Si K emission-band spectra

The Si K emission-band spectra are expected to reflect the density of Si p states below the Fermi level. For the $3d$ TM disilicides the experimental spectra and Si p DOS are compared in Fig. 4. The spectra are dominated by peaks at about 2.5 to $\sim$5 eV, but do have in addition some weak structures and shoulders. The agreement between the shape of the spectra and the partial DOS is good, but on close inspection there are significant differences. Thus, for instance, we see that for $CoSi_2$ and $NiSi_2$ the partial DOS peaks are, respectively, 0.3 and 0.5 eV higher in BE than found in experiment (see also Table II). This is the sort of difference we would attribute to self-energy effects.[36] In another case, in $CrSi_2$, the Si p DOS show a splitting of $\sim$2.9 eV, which is much larger than that apparent in the spectrum ($\sim$1.6 eV). Again, this may be due to self-energy effects, but the difference is rather large. Both these differences mentioned above are too large to be attributed entirely to energy dependence of matrix elements.

There are two general trends found in both p DOS and K emission-band spectra of the TM disilicides which should be noted. The first is that in all cases the weight of the Si p DOS or of the spectrum falls off as one approaches E_F. This effect is too large to be attributed to the spectral resolution and lifetime broadening alone. It is a consequence of the interaction between Si p and metal d states and is often referred to in the literature as a quasigap.[3,4,37] This will be explained further in Sec. V F. The second trend is the shift of the Si p peak to higher BE as the TM d band is filled and also moves to higher BE. The origin of these shifts will be discussed in Sec. V F.

F. Shifts as a function of TM d band filling

In the preceding sections we noted several trends in our data as a function of the occupation number of the $3d$ transition metal in the silicides we have measured. If we consider the sequence $TiSi_2 \rightarrow NiSi_2$, then these trends are (i) a shift of the experimentally observed Si s peak position of $\sim$2.1 eV to higher binding energies (Fig. 1); (ii) in the calculated and unbroadened DOS (only broadened curves are shown in Fig. 1) we observe a shift of the bottom of the Si s band of $\sim$2.0 eV to higher binding energies, (iii) a shift of the Si p peak position of $\sim$2.4 eV, also to higher binding energies (Fig. 4); (iv) a shift of the TM d peak position of $\sim$2.4 eV to higher binding energies. This peak shift is deduced from the DOS calculations only (Fig. 5), but is confirmed experimentally by XPS measurements;[2] (v) For the $4d$ TM disilicides we do not have such an extended series of measurements, but the trends summarized in the points (i)–(iii) have the same direction in going from $NbSi_2$ to $MoSi_2$. In order to put these results in a context we turn to Fig. 6, which is taken from Ref. 6. In that paper we discussed the interaction between TM d and Si sp states and presented a scheme of chemical bonding in TM silicides. To give a brief summary of those results we can say that a strong concentration of Si s states between 6 and 13 eV below E_F is found in all TM silicides. (See Ref. 30, and Figs. 1–3.) At higher energies, i.e., between 2 and 7 eV below E_F, a concentration of Si p states is found (Fig. 4). Next, a quasigap opens up which extends to $\sim$2 eV above E_F, but in which still an appreciable amount of Si s and p character is located. Above this quasigap a second peak of Si p character, but of also some Si s character, is found. The TM d states are centered in this quasigap, but overlap strongly with the two peaks of Si p character on either

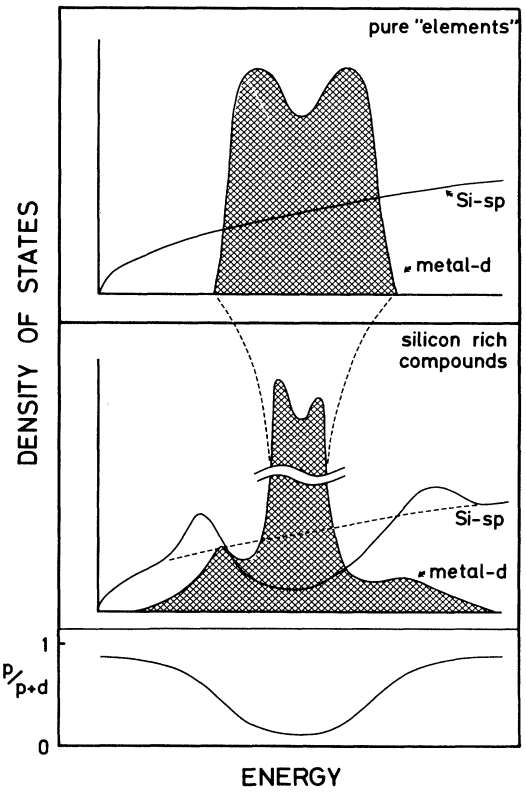

FIG. 6. Schematic illustration of the electronic structure of TM silicides. The upper frame indicates the DOS of the elements without mutual interaction. In the lower frame the effects of the interaction are shown. See text for explanation.

side of the quasigap, resulting in regions which give above and below the quasigap, respectively, bonding and antibonding forces between Si and TM atoms. To put it more strongly, the quasigap is a direct result of the interaction of the TM d states with the Si sp band; results of DOS calculations for the hypothetical case of silicon in a TM silicide lattice without metal atoms[38] do not show a quasigap.[3] The TM d states that are located in the quasigap also contribute to the chemical bonding via direct TM-TM interaction. This d-d overlap results in a bonding and antibonding region within the TM d band itself.

Several features of this general framework can be recognized in the experimental spectra presented here. For instance, the sequence of levels, i.e., Si $s \rightarrow$ Si $p \rightarrow$ TM d, can easily be recognized in Figs. 4 and 5. Furthermore, both the Si $L_{2,3}$ and K emission bands have a low spectral intensity at the Fermi level which can be ascribed to a low DOS, due to the quasigap. Also in other cases we found a low spectral intensity near E_F in the Si p DOS,[6,7] thus confirming the existence of the Si quasigap. The Si p states below E_F can be characterized as being bonding states. Centered in this quasigap lies the TM d band and the occupation number of this d band determines the position of E_F. This statement is confirmed by the observation of the peak shifts in the emission spectra, summarized in the points (i)–(iii) at the beginning of this section. Obviously, the TM d states do interact strongly with the Si p states and less strongly with the Si s states. This explains the shift of the Si s peaks and the shift of the bottom of the Si s band.

Hybridization of the TM d states with the Si p band leads to some structure in the Si K emission spectra. In $TiSi_2$ most of the metal d band is unoccupied and therefore the Si K emission spectrum only shows an unstructured peak, fairly close to E_F. In the K emission spectrum of $CrSi_2$, but especially in the one of $CoSi_2$, the effect of hybridization is clearly visible as more structure appears in the spectra. In $NiSi_2$ the metal d band is nearly completely occupied, causing the Fermi level to be positioned at the top of the Si quasigap, and the antibonding Si s states become visible as a small but sharp peak just below E_F (Fig. 1).

G. Trends as a function of composition

The composition of the TM silicides has a strong influence on the chemical bonding and hence on the distribution of the DOS, which can be seen clearly in Fig. 2. As a function of increasing silicon content, i.e., the sequence $Cr_3Si \rightarrow CrSi_2$, we can observe three trends. The first one is a shift of the main peak to lower binding energies. The highest peak in the spectrum of $CrSi_2$ also follows this trend, but if we take the centroid of this double peak then the trend is broken. In Sec. V F we already pointed out the indirect influence of the TM d states on the Si s states and we believe that this peak shift can be explained in a similar way: Simultaneously with the decreasing chromium contents the Cr d–Cr d interaction decreases and hence also the Cr $3d$-band width. Although the centroid of this band remains unchanged, the hybridization with the Si p states extends to lower binding energies, which causes these states to be centered at low binding energies as well. From the interaction between Si p and Si s states follows the shift which is observed in Fig. 2.

The second trend, following the same sequence as above, is the increasing FWHM of the Si s peak. The increasing Si contents induces more and stronger overlap of the Si s (and p) orbitals because the number of nearest neighbors increases and simultaneously their distances decrease. From this stronger overlap a broader Si s band follows directly.

Finally, the third trend is the increasing intensity of the plateau region near E_F. However, no conclusion can be drawn from this because the spectra are normalized to a constant height. Normalization to a constant surface underneath the spectra did not show a significant trend in the plateau region intensity.

H. Self-energy effects

We have drawn attention to various differences between experimental spectra and partial DOS calculations in several preceding sections. Our purpose here is to collect together those differences which should be further investigated with respect to the contribution of self-energy. We distinguish here three potential causes of differences between calculated partial DOS curves and measured spectra.

1. Single-particle matrix elements

The influence of the single-particle matrix elements has not been extensively investigated although Schwarz *et al.*[21,22] performed APW calculations at the beginning of the 1980s and they report important matrix-element effects. These effects arise because the difference in electron density at the Wigner-Seitz radius for bonding and antibonding levels leads to renormalization of the electron densities associated with the valence states in the core region of the $1s$ or $2p$ wave functions. This in turn leads to differences in the strength of the matrix elements $|\langle \phi_f | t | \phi_i \rangle|^2$. However, one would not expect these effects to be terribly strong because the states at the bottom of the bands are normally bonding and have a maximum in the electron density close to the Wigner-Seitz boundary. Their weight in the core region is minimized and hence the matrix element too is smaller than for the antibonding states at the top of the bands.

2. Real and imaginary parts of the self-energy

The self-energy effects may be divided into a real and an imaginary part, giving rise to, respectively, a shift and a broadening of the spectral features with respect to the calculated partial DOS curves. There are major differences in the shape of the large Si s state peak $\sim$7–10 eV below E_F, for several but not all of the silicides studied (i.e., all the disilicides and CrSi, but not $MoSi_2$). In some cases, the differences are much larger

than those we normally associate with self-energy effects, e.g., in $CrSi_2$ and $NbSi_2$. If we take the latter as an example to analyze in detail, i.e., $NbSi_2$ of Fig. 3, then we see that there the peak is shifted by nearly 1 eV and in the experimental spectrum the double-peak structure of the calculated DOS is only recognizable as a strong peak with a weak shoulder at its low binding energy side. Although implementation of energy-dependent transition matrix elements would decrease the calculated DOS intensity at the bottom of the band and hence would lead to a better match between the calculated and measured intensities, it never can induce large peak shifts which would be necessary in addition to eliminate the large differences observed.

Second, the imaginary part of the self energy, i.e., the lifetime broadening, is high at the bottom of the band and this also tends to depress the intensity in that region. In our simulations we assume a 12% FWHM (i.e., increasing linearly with the binding energy), which is based on experience but is not necessarily correct. For example, in semiconductors jumps in the real part of the self-energy corrections are reported by Jackson and Allen[39] and this also seems to be the case in our spectra. Jumps in the imaginary part within the Si s band might also be possible and would result in a stronger effect in the lifetime broadening corrections than the 12% we used. If so, the effects are larger than normal. Abrupt changes in the self-energy corrections are expected whenever the character of states changes and are especially important for highly localized electrons[39] (such as $4f$ states, etc.), but not for Si $3s$ states because these states are too extended. This subject clearly needs more investigation.

I. Relevance of self-energy effects for metal-silicon interfaces

Most theoretical calculations at metal-silicon interfaces use the local-density approximation (LDA) and in terms of the spectral studies they suffer the same problems as do bulk calculations, i.e., they are not calculations of excited states and the self-energy contribution must be envisaged. The large differences between DOS and experiments found here indicate that such computations could be very different for surface and interface states also. However, there is a second motivation for such calculations, namely to give insight into the height of the Schottky barrier (SB) and we are not sure if self-energy effects may actually be important here too. Normally one assumes that the SB height is defined mainly by the total electron density distribution and this should be given correctly by LDA calculations. Also it is generally considered that LDA calculations should give correctly at least the one lowest ionization potential. However, metal-silicon interface formation lead to formation or rejection of new metal-induced gap states (MIGS) into the Si band gap, and these are believed to pin the Fermi level and hence the SB in many cases.[40] We do know that LDA calculations underestimate the semiconductor band gap by a factor of 2 due to self-energy[41,42] and now we find in some of these silicides large differences between DOS and experiment which also may be due to self-energy effects. Thus we would not be surprised if the order of some of these MIGS would have been strongly shifted within the semiconductor band gaps by self-energy effects. This would produce problems in calculating SB heights, such as those found by Das *et al.*,[43] for example.

VI. CONCLUDING REMARKS

In this paper we presented XES results for various TM silicides. Until now, the Si s and p states of these silicides were only directly measured by some studies. Our results complete the existing experimental data and confirm our scheme of chemical bonding which is extensively discussed in Ref. 6 and in Sec. V E. A summary of the conclusions from Sec. V can be given as follows.

(1) In the Si $L_{2,3}$ emission-band spectra both the Si s and d state densities contribute significantly to the spectral intensity in the low BE region (Sec. V A). These Si d states are in some way linked to the tails of the TM d wave functions (Sec. V B).

(2) The shape of the Si s state peaks show considerable differences for different silicides (Sec. V C). These states contribute to the bond order and cohesive energy. Furthermore, the Si configuration is approximately $s^{1.6}p^{2.4}$ (Sec. V D).

(3) Both Si s and p states have a low DOS at the Fermi level, due to the quasigap (Secs. V D and V E). The Si s and p peaks shift to higher BE as the TM d band gets more occupied (Sec. V F).

(4) The composition of the TM silicides influences the chemical bonding and hence the density distribution of the Si s (and p) states (Sec. V G). A decreasing TM contents induces broader Si s bands and a shift of these bands to lower binding energies.

(5) In Sec. V H we tentatively explained the differences between the calculated DOS and the experimental spectra in terms of self-energy effects. Some of these differences can be understood quite well, but there are still subjects which need more investigations. We further discussed the point that similar effects might be important in any computation of the electronic structure of metal-semiconductor interfaces.

---

*Present address: Philips Research Laboratories, P.O. Box 80.000, NL-5600 JA Eindhoven, The Netherlands.

†Present address: Natuurkundig Laboratorium, Vrije Universiteit, P.O. Box 7161, NL-1007 MC Amsterdam, The Netherlands.

[1]D. D. Sarma, W. Speier, L. Kumar, C. Carbone, A. Spinsanti, O. Bisi, A. Iandelli, G. L. Olcese, and A. Palenzona, Z. Phys. B **71**, 69 (1988).

[2]W. Speier, J. C. Fuggle, P. Durham, R. Zeller, R. J. Blake, and P. Sterne, J. Phys. C **21**, 2621 (1988).

[3]D. D. Sarma, W. Speier, R. Zeller, E. van Leuken, R. A. de Groot, and J. C. Fuggle, J. Phys.: Condens. Matter **1**, 9131

(1989).
[4]W. Speier, E. van Leuken, J. C. Fuggle, D. D. Sarma, L. Kumar, B. Dauth, and K. H. J. Buschow, Phys. Rev. B **39**, 6008 (1989).
[5]W. Speier, L. Kumar, D. D. Sarma, R. A. de Groot, and J. C. Fuggle, J. Phys.: Condens. Matter **1**, 9117 (1989).
[6]P. J. W. Weijs, M. T. Czyżyk, J. C. Fuggle, W. Speier, D. D. Sarma, and K. H. J. Buschow, Z. Phys. B **78**, 423 (1990).
[7]P. J. W. Weijs, M. T. Czyżyk, J. F. van Acker, W. Speier, J. B. Goedkoop, H. van Leuken, H.J. M. Hendrix, R. A. de Groot, G. van der Laan, K. H. J. Buschow, G. Wiech, and J. C. Fuggle, Phys. Rev. B **41**, 11 899 (1990).
[8]P. J. W. Weijs, G. Wiech, W. Zahorowsky, W. Speier, J. B. Goedkoop, M. Czyżyk, J. F. van Acker, E. van Leuken, R. A. de Groot, G. van der Laan, D. D. Sarma, L. Kumar, K. H. J. Buschow, and J. C. Fuggle, Phys. Scr. **41**, 629 (1990).
[9]For exhaustive reviews see L. J. Brillson, Surf. Sci. Rep. **2**, 123 (1982), or C. Calandra, O. Bisi, and G. Ottaviani, Surf. Sci. Rep. **4**, 271 (1985), and references therein.
[10]G. W. Rubloff, Surf. Sci. **132**, 268 (1983).
[11]R. Butz, G. W. Rubloff, T. Y. Tan, and P. S. Ho, Phys. Rev. B **30**, 5421 (1984).
[12]J. H. Weaver, A. Franciosi, and V. L. Morruzi, Phys. Rev. B **29**, 3293 (1984).
[13]A. Franciosi, J. H. Weaver, and D. G. O'Neill, Phys. Rev. B **28**, 4889 (1983).
[14]W. Zahorowski, J. Mitternacht, and G. Wiech, Meas. Sci. Technol. **2**, 602 (1991).
[15]E. Zöpf, Ph.D. thesis, Ludwig-Maximillians Universität, München, 1972.
[16]A. R. Williams, J. Kübler, and C. D. Gelatt, Jr., Phys. Rev. B **19**, 6094 (1979).
[17]M. O. Krause and J. H. Oliver, J. Phys. Chem. Ref. Data **8**, 329 (1979).
[18]J. C. Fuggle and S. F. Alvarado, Phys. Rev. A **22**, 1615 (1980).
[19]D. van der Marel, G. A. Sawatzky, R. Zeller, F. U. Hillebrecht, and J. C. Fuggle, Solid State Commun. **50**, 47 (1984).
[20]W. Speier, R. Zeller, and J. C. Fuggle, Phys. Rev. B **32**, 3597 (1985).
[21]K. Schwarz and E. Wimmer, J. Phys. F **10**, 1001 (1980).
[22]K. Schwarz, H. Ripplinger, and A. Neckel, Z. Phys. B **48**, 79 (1982).
[23]M. Iwami, M. Kusaka, M. Hirai, H. Nakamura, K. Shibahara, and H. Matsunami, Surf. Sci. **199**, 467 (1988).
[24]R. S. Crisp, D. Haneman, and V. Chacorn, J. Phys. C **21**, 975 (1988).
[25]G. Wiech, W. Zahorowsky, A. Šimůnek, and O. Šipr, J. Phys.: Condens. Matter **1**, 5595 (1989).
[26]H. Nakamura, M. Iwami, M. Hirai, M. Kusaka, F. Akao, and H. Watabe, Phys. Rev. B **41**, 12 092 (1990).
[27]E. Belin, C. Senemaud, L. Martinage, J. Y. Veuillin, D. A. Papaconstantopoulos, A. Pasturel, and F. Cyrot-Lackmann, J. Phys.: Condens. Matter **2**, 3247 (1990).
[28]K. Tanaka, T. Saito, K. Suzuki, and R. Hasegawa, Phys. Rev. B **32**, 6853 (1985).
[29]W. Zahorowski, A. Šimůnek, G. Wiech, K. Söldner, R. Knauf, and G. Saemann-Ischenko, J. Phys. (Paris) Colloq. **9**, C-1025 (1987).
[30]G. Wiech and E. Zöpf, in *Band Structure Spectroscopy of Metals and Alloys,* edited by D. J. Fabian and L. M. Watson (Academic, London, 1973), p. 173.
[31]K. Söldner, A. Grassmann, G. Saemann-Ischenko, W. Zahorowski, A. Šimůnek, and G. Wiech, Z. Phys. B **75**, 59 (1989).
[32]Ch. Beyreuther and G. Wiech, Phys. Fenn. **9**, **S1**, 168 (1974).
[33]V. I. Anisimov, A. V. Postnikov, E. Z. Kurmaev, and G. Wiech, Phys. Met. Metallogr. (USSR) **62**, 96 (1986).
[34]This correlation is made stronger by the observation that the ratio of the TM *d* expectation radius to the Wigner-Seitz radius also decreases in the sequence Ti→Ni. See D. van der Marel, Ph.D. thesis, Groningen University, 1985; and J. C. Fuggle, in *Narrow Band Phenomena,* edited by J. C. Fuggle, G. A. Sawatzky, and J. W. Allen (Plenum, New York, 1988), p. 3.
[35]K. Okuno, M. Iwami, A. Hiraki, M. Matsumura, and K. Asayama, Solid State Commun. **33**, 899 (1980).
[36]We note that Belin *et al.* did find a very good agreement between experimental and calculated peak positions of Si *p* DOS in $CoSi_2$, but also a difference of 0.2 eV in the position of the shoulder at the lower binding energy: E. Belin, C. Senemaud, L. Martinage, J. Y. Veuillen, D. A. Papaconstantopoulos, A. Pasturel, and F. Cyrot-Lackmann, J. Phys.: Condens. Matter. **2**, 3247 (1990).
[37]J. Tersoff and D. R. Hamann, Phys. Rev. B **28**, 1168 (1983).
[38]The Si DOS in a FeSi lattice without Fe is calculated by R. A. de Groot (private communication). The Si DOS in a $NiSi_2$ lattice without Ni is calculated by G. P. Das (private communication).
[39]W. B. Jackson and J. W. Allen, Phys. Rev. B **37**, 4618 (1988).
[40]P. J. W. Weijs, J. F. van Acker, J. C. Fuggle, P. A. M. van der Heide, H. Haak, and K. Horn, Surf. Sci. (to be published).
[41]R. W. Godby, M. Schlüter, and L. J. Sham, Phys. Rev. B **37**, 10 159 (1988).
[42]R. W. Godby and R. J. Needs, Phys. Rev. Lett. **62**, 1169 (1989).
[43]G. P. Das, P. Blöchl, O. K. Andersen, N. E. Christensen, and O. Gunnarsson, Phys. Rev. Lett. **63**, 1168 (1989).
[44]*Structure Reports,* edited by J. Trotter (International Union of Crystallography, Bohn and Schelten at Holkena, Utrecht), Vol. 7, pp. 12 and 95.
[45]*Structure Reports* (Ref. 44), Vol. 8, p. 112.
[46]*Structure Reports* (Ref. 44), Vol. 13, p. 90.
[47]*Structure Reports* (Ref. 44), Vol. 3, p. 14.
[48]*Structure Reports* (Ref. 44), Vol. 20, p. 78.
[49]*Structure Reports* (Ref. 44), Vol. 38A, p. 98.
[50]*Structure Reports* (Ref. 44), Vol. 1, p. 783.